DOI: 10.1002/chem.200901408

Microwave-Assisted Functionalization of Carbon Nanostructures in Ionic Liquids

Ivan Guryanov,[a] Francesca Maria Toma,[b, d] Alejandro Montellano López,[b] Mauro Carraro,[a] Tatiana Da Ros,[b] Guido Angelini,[c] Eleonora D'Aurizio,[c] Antonella Fontana,*[c] Michele Maggini,*[a] Maurizio Prato,*[b] and Marcella Bonchio*[a]

Dedicated to the Centenary of the Italian Chemical Society

Abstract: The effect of microwave (MW) irradiation and ionic liquids (IL) on the cycloaddition of azomethine ylides to [60]fullerene has been investigated by screening the reaction protocol with regard to the IL medium composition, the applied MW power, and the simultaneous cooling of the system. [60]Fullerene conversion up to 98 % is achieved in 2–10 min, by using a 1:3 mixture of the IL 1-methyl-3-*n*-octyl imidazolium tetrafluoroborate ([omim]BF_4) and *o*-dichlorobenzene, and an applied power as low as 12 W. The mono- versus poly-addition selectivity to [60]fullerene can be tuned as a function of fullerene concentration. The reaction scope includes aliphatic, aromatic, and fluorous-tagged (FT) derivatives. MW irradiation of IL-structured bucky gels is instrumental for the functionalization of single-walled carbon nanotubes (SWNTs), yielding group coverages of up to one functional group per 60 carbon atoms of the SWNT network. An improved performance is obtained in low viscosity bucky gels, in the order [bmim]$BF_4 >$ [omim]$BF_4 >$ [hvim]TF_2N (bmim = 1-methyl-3-*n*-butyl imidazolium; hvim = 1-vinyl-3-*n*-hexadecyl imidazolium). With this protocol, the introduction of fluorous-tagged pyrrolidine moieties onto the SWNT surface (1/108 functional coverage) yields novel FT-CNS (carbon nanostructures) with high affinity for fluorinated phases.

Keywords: cycloaddition · fullerenes · ionic liquids · microwave chemistry · nanotubes

Introduction

Research on carbon nanostructures (CNS), such as fullerenes, carbon nanotubes, and graphene, has recently been the focus for scientists from many disciplines, owing to their exclusive structures and properties. Shortly after their discovery, the fullerenes were subjected to extensive studies of chemical modification to understand their reactivity and to tune their properties.[1] Exohedral addition of organic groups helps to control solubility, morphology in the solid state, and electronic properties of the fullerene core. The azomethine ylide cycloaddition, yielding fulleropyrrolidines (FPs),[2] has contributed significantly to the development of new nanocarbon-based materials for strategic fields such as solar energy conversion or molecular medicine.[3] FP synthesis tolerates many functional groups and is significantly accelerated by microwave (MW) irradiation.[4,5] Several FPs have been prepared under MW irradiation by Langa and coworkers, with yields up to 37 % and interesting regioselectivities in the case of additions to C_{70}.[4] In these reactions, toluene, benzene, or *o*-dichlorobenzene (*o*-DCB) have been

---

[a] Dr. I. Guryanov, Dr. M. Carraro, Prof. M. Maggini, Dr. M. Bonchio
ITM-CNR and Department of Chemical Sciences
University of Padova
Via Marzolo, 1, 35131 Padova (Italy)
Fax: (+39) 049-8275239
E-mail: michele.maggini@unipd.it
marcella.bonchio@unipd.it

[b] Dr. F. M. Toma, Dr. A. Montellano López, Dr. T. Da Ros,
Prof. M. Prato
Dipartimento di Scienze Farmaceutiche, INSTM unit of Trieste
Piazzale Europa 1, 34127 Trieste (Italy)
Fax: (+39) 040-52572
E-mail: prato@units.it

[c] Dr. G. Angelini, Dr. E. D'Aurizio, Prof. A. Fontana
Dipartimento di Scienze del Farmaco
Università "G. d'Annunzio"
Via dei Vestini, 66013 Chieti (Italy)
Fax: (+39) 0871-3554461
E-mail: fontana@unich.it

[d] Dr. F. M. Toma
SISSA
Via Beirut 2-4, 34151 Trieste (Italy)

Supporting information for this article is available on the WWW under http://dx.doi.org/10.1002/chem.200901408.

used as solvents, although *o*-DCB should be preferred for fullerene solubility, efficient microwave absorption, and relatively high boiling point.

Building on the fullerene experience, a wide variety of reactions have been also described for the covalent functionalization of carbon nanotubes (NTs). At variance with the fullerene analogues, NTs require harsh temperature and/or pressure conditions, with greater use of organic solvents, and long reaction times. Therefore, MW-assisted and solvent-free protocols have been developed to accelerate reactions and produce functionalized NTs efficiently. A recent achievement was the double functionalization of single-walled carbon nanotubes (SWNTs) with azomethine ylides and arene radical additions, both promoted by MW irradiation.[6] In this perspective, the optimization of functionalization methods for CNS should also address the replacement of hazardous volatile organic solvents with alternative reaction media. To this end, room-temperature ionic liquids (ILs) have been used successfully for a variety of organic transformations.[7] Recognized advantages of ILs are their tunable composition, polar character, non-volatility, thermal resistance, complementarity with water or other green media, and liquid electrolyte behavior. In addition, IL phases are instrumental for fast and selective MW heating by the ionic conduction mechanism, with negligible vapor pressure and safer setup conditions.[8] The combination of ILs and CNS has hardly been explored, with just a few reports related to the synthesis of methanofullerenes[9] and hydrogenation reactions.[10] Aggregation phenomena, driven by the low solubility of CNS in polar environments, are expected to affect the reactivity behavior in IL media. Notably, it has recently been discovered that SWNTs, upon grinding with IL, form highly viscous gels termed "bucky gels", the thermal,[11] electrochemical,[12] and rheological properties[13] of which have been investigated by several authors. The gelation refers to mixtures in which an exfoliation process of nanotube bundles is induced by the tendency of the IL to adsorb onto the SWNT surface. The use of bucky gels as reaction media has been investigated for the addition of diazonium ions to the SWNT surface.[14] Exfoliation of the SWNT ropes by the IL environment accelerates the reaction, which occurs in minutes at room temperature.

In this work, we investigate the effect of MW irradiation and ILs on the cycloaddition of azomethine ylides to [60]fullerene and CNTs by screening the reaction protocol in relation to the IL medium composition, the concentration factor, the applied MW power, and the simultaneous cooling of the system. This latter turned out to be crucial for directly dosing high levels of MW power to the reaction without overheating.[15] Our results include: 1) the evaluation of the cycloaddition kinetics and selectivity in both *o*-DCB- and IL-containing media; 2) optimization of the synthetic protocol towards multisubstitution on the fullerene core and the CNT surface; 3) examination of the reaction scope, with both aliphatic and aromatic aldehydes; 4) extension of the optimized protocol to fluorous-tagged aldehydes. Under MW-assisted conditions in IL phases, fluorous-tagged CNS (FT-CNS) could be readily isolated. Preliminary investigations showed a remarkable solubility of FT-CNS in fluorous phases, with potential applications in catalysis, material science, and membrane-based technology.[16]

Results and Discussion

Synthesis of [60]fullerropyrrolidines in IL media under MW irradiation: The reactivity of [60]fullerene was considered first, as an evaluation benchmark to test and optimize the conditions for an efficient functionalization of CNS by MW-induced flash heating in IL phases. In particular, we focused on the use of MW-activated IL phases to accelerate the thermal azomethine ylide cycloaddition, while providing an additional tool for tuning the selectivity outcome of the polyadduct distribution (Scheme 1). A key observation was that cycloreversion of FPs could be readily achieved in IL under MW irradiation within minutes, by unlocking the pyrrolidine ring to back-release pristine [60]fullerene.[17] No other additive is required, as the IL solvates the incipient 1,3-dipole by electrostatic interactions, while the MW-induced dielectric heating speeds up the thermal cycloreversion with unprecedented rates.[17,18] As a matter of fact, in pure IL media, cycloreversion turned out to be the dominating process, because [60]fullerene, which is hardly soluble in such a polar environment, precipitates, thus hampering the thermodynamic equilibration of the reagent/product distribution. In pure IL, functionalization of [60]fullerene failed to yield any cycloadduct, regardless of the IL type, applied MW power, and irradiation time (entry 1, Table 1). However, when *o*-DCB is used as a co-solvent, the rate of retro-cycloaddition is remarkably slowed down.[17]

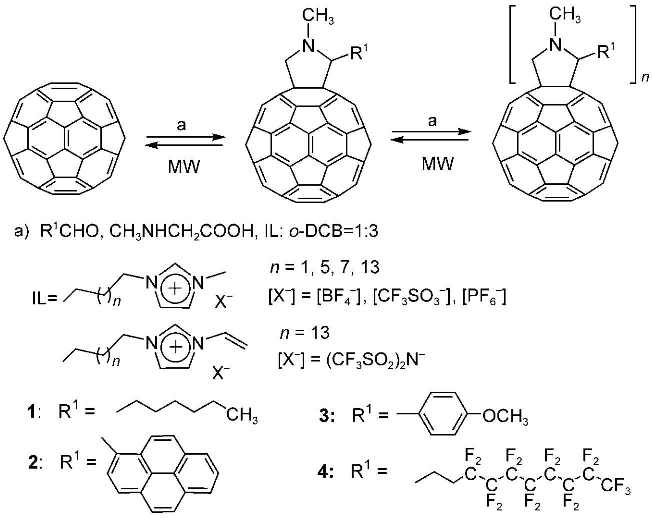

Scheme 1. Azomethine ylide cycloadditions to [60]fullerene yielding mono- and poly-adducts under MW irradiation, in IL/*o*-DCB mixtures.

Therefore, the best solvent composition was set for the synthesis of model FPs **1** by changing the relative IL/*o*-DCB

Table 1. Effect of [omim]BF_4/*o*-DCB ratio on the yield and selectivity of mono- and poly-FPs **1**, obtained by MW-assisted reaction of [60]fullerene with sarcosine and heptaldehyde.

Entry[a]	IL/*o*-DCB	Conv. [%][b]	Mono-FP [%][c]	Selectivity[d]
1[e]	1/0	–	–	–
2[e]	4/1	18	6	0.5
3[e]	2/1	21	9	0.8
4[e]	1/1	64	22	0.5
5[e]	1/2	58	21	0.6
6[e]	1/3	60	30	1
7[f]	1/3	64	44	2.2
8[f]	1/9	52	38	3.0
9[f,g]	0/1	15	15	–

[a] In all reactions: [60]fullerene 0.14 mmol; sarcosine 0.28 mmol; heptaldehyde 0.56 mmol; MW irradiation at 12 W, 10 min, $T_{bulk} = 100$ °C, under magnetic stirring and simultaneous cooling by compressed air. [b] [60]Fullerene conversion monitored by HPLC analysis. [c] % of mono-FP **1** monitored by HPLC analysis. [d] Mono-FP/poly-FP ratio. [e] Reaction performed in 0.5 mL. [f] Reaction performed in 1.0 mL. [g] MW irradiation at 20 W.

Table 2. Effect of the IL nature on the yield and selectivity of mono- and poly-FPs **1**, obtained by MW-assisted reaction of [60]fullerene with sarcosine and heptaldehyde.

Entry[a]	IL[b]	Conv. [%][c]	Mono-FP **1** [%][d]	Selectivity[e]
1[f]	[bmim]BF_4	25	17	2.1
2[g]	[bmim]BF_4	15	15	–
3[f]	[bmim]PF_6	9	9	–
4[f]	[omim]BF_4	46	18	0.6
5[g]	[omim]BF_4	58	43	2.9
6[f]	[omim]CF_3SO_3	56	13	0.3
7[g]	[omim]CF_3SO_3	52	38	2.7
8[f]	[dmim]BF_4	35	19	1.2
9[g]	[dmim]BF_4	44	34	3.4
10[g]	[hmim]PF_6	44	33	3.0
11[g]	[hvim][$(CF_3SO_2)_2N$]	60	41	2.2

[a] In all reactions: [60]fullerene 0.07 mmol; sarcosine 0.14 mmol; heptaldehyde 0.28 mmol; MW irradiation at 12 W, 3–5 min, $T_{bulk} = 100$ °C, under magnetic stirring and simultaneous cooling by compressed air. [b] 1-Methyl-3-*n*-butyl imidazolium [bmim], 1-methyl-3-*n*-octyl imidazolium [omim], 1-methyl-3-*n*-decyl [dmim], 1-methyl-3-*n*-hexadecyl [hmim], 1-vinyl-3-*n*-hexadecyl [hvim]. [c] [60]Fullerene conversion monitored by HPLC analysis. [d] % of mono-FP **1** monitored by HPLC analysis. [e] Mono-FP/poly-FP ratio. [f] Reaction performed in 0.5 mL. [g] Reaction performed in 1.0 mL.

content and optimizing the overall [60]fullerene conversion (Table 1). In this preliminary screening, 1-methyl-3-*n*-octyl imidazolium tetrafluoroborate ([omim]BF_4) was used because it gives finer fullerene dispersions than other imidazolinium-based ILs.[19] Interestingly, under MW irradiation at 12 W, $T_{bulk} = 100$ °C for 10 min, the change in solvent composition in favor of *o*-DCB leads to a steady increase of the overall yield and of the mono-substitution selectivity (entries 1–6, Table 1). This latter turned out to be remarkably affected by the relative solubility of reagents and products in the solvent system, which is mainly controlled by the IL content and by the [60]fullerene concentration. Indeed, an unexpected prevalence of polyadducts (mono-FP/poly-FP < 1) was registered at IL > 25 % (entries 2–6, Table 1). In addition, the selectivity reverts in favor of the monoadduct upon dilution (compare entries 6 and 7, Table 1). For the IL-free reaction, which lacks the ionic absorbing component, the accelerating effect of MW irradiation (even at MW power = 20 W) is very poor (Table 1, entry 9). The results reported in Table 1 indicate that the phase in which IL/*o*-DCB = 1:3 guarantees both a fast reaction and a convenient selectivity control, which, possibly, depends on clustering/aggregation phenomena. Further insight into the interplay of such factors for selectivity tuning has been obtained from kinetic studies (vide infra).

With the aim of optimizing the reaction protocol, a series of ILs were screened as co-solvents for the MW-assisted FP **1** reference reaction (Table 2). Alkyl imidazolium ILs, butyl ([bmim]$^+$), octyl ([omim]$^+$), decyl ([dmim]$^+$), hexadecyl ([hmim]$^+$) and hexadecylvinyl ([hvim]$^+$) (Scheme 1), were evaluated to highlight the impact of the alkyl chain length on FP **1** synthesis. Different counteranions, $[BF_4]^-$, $[CF_3SO_3]^-$, $[PF_6]^-$, and $[(CF_3SO_2)_2N]^-$ were also considered as their role in controlling the hydrophilicity/hydrophobicity properties of IL media is well known.[7]

Both [60]fullerene conversion and addition selectivity (mono- versus polyaddition) depend on the IL nature. In particular, conversions in the 40–60 % range are achieved in 3–5 min with ILs bearing long alkyl chains (entries 4–11, Table 2). Selectivity, on the other hand, seems once again governed by the solubility of fullerenes in the reaction medium. Values of 3.4 for the mono-FP/poly-FP ratio were obtained (entry 9, Table 2). This compares well with the results recorded under diluted conditions (Table 1). Apparently, the IL counteranion plays a minor role in this chemistry. From the data reported in Table 2, [omim]BF_4 is the best hit in terms of conversion yield and selectivity for FPs **1** synthesis. Figure 1 shows the time evolution profile of mono- and poly-FPs **1** in [omim]BF_4/*o*-DCB = 1:3, and the comparison with the IL-free reaction setup. The combined use of IL and MW, even at applied power as low as 12 W, is responsible for a remarkable acceleration of the reaction, leading to

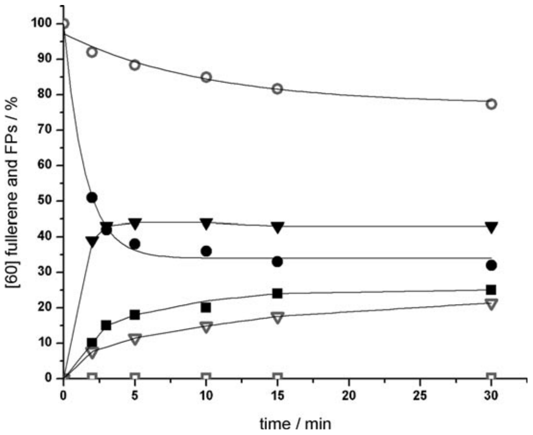

Figure 1. Kinetics of [60]fullerene conversion (circles) to mono- and poly-FPs **1** (triangles and squares, respectively) by 1,3-dipolar cycloaddition of sarcosine, and heptaldehyde in 1 mL of *o*-DCB (empty symbols) or in [omim]BF_4:ODCB = 1:3 (filled symbols) under MW irradiation (see conditions in Table 1).

mono-FP **1** with a plateau yield >40%, after only 3 min under MW irradiation. This finding is important for the potential upgrade of the azomethine ylide synthesis under continuous flow conditions using microfluidic technology.[20] Yield optimization was also investigated by varying the relative ratio of the azomethine ylide precursors, sarcosine and heptaldehyde, and their additional recharge during the reaction that, in turn, was carried out at different [60]fullerene concentrations (Table 3). Under the optimal conditions for monoaddition, the yield of mono-FP **1** levels off at ≈40%, with no major effects of reagent recharging (entries 4–6, Table 3). Such limiting yield is probably attributable to equilibrium constraints, which dictate the observed product distribution, as a result of the thermally activated retro-cycloaddition involving both mono- and poly-FP.[17,18]

Table 3. Effect of sarcosine/heptaldehyde equivalent ratio on the yield and selectivity of mono- and poly-FPs **1**, obtained by MW-assisted cycloaddition to [60]fullerene.

Entry[a]	Sarcosine/ heptaldehyde[b]	Conv. [%][c]	Mono-FP [%][d]	Selectivity[e]
1[f]	1/1	34	16	0.9
2[f]	2/4	60	30	1
3[f]	10/20	95	4	0.04
4[g]	2/4	58	42	2.9
5[g]	4/8	69	44	1.8
6[g,h]	2/4+2/4	72	41	1.3

[a] In all reactions: [60]fullerene 0.14 mmol; [omim]BF_4/o-DCB = 1/3; MW irradiation at 12 W, 10 min, T_{bulk} = 100 °C, under magnetic stirring and simultaneous cooling by compressed air. [b] Added equivalents with respect to [60]fullerene. [c] [60]Fullerene conversion monitored by HPLC analysis. [d] % of mono-FP **1** monitored by HPLC analysis. [e] Mono-FP/poly-FP ratio. [f] Reaction performed in 0.5 mL. [g] Reaction performed in 1.0 mL, in 3 min. [h] Added in two portions in 4 min.

A fast and quantitative conversion of pristine [60]fullerene to FP **1** polyadducts became accessible at a fullerene concentration equal to 0.28 M (see the kinetic plot in the Supporting Information, Figure S1) and excess (10/20-fold) of sarcosine and heptaldehyde (entry 3, Table 3). The reaction scope is highlighted in Table 4. In all cases, monosubstitution occurs with good to excellent selectivities in just 2 min of MW irradiation, with a top performance registered for the *p*-methoxyphenyl derivative (entry 3 in Table 4). Notably, in the reaction with pyrene aldehyde, poly-FPs **2** are the major products regardless of the sarcosine/aldehyde excess and of the MW irradiation time (entries 2 and 6, Table 4). This latter observation can be addressed on the basis of the poor cycloreversion tendency exhibited by pyrene-substituted FPs in IL phases, under MW-activated conditions.[17] The thermal stability of such cycloadducts prevents the back-release of [60]fullerene and its equilibration to both mono- and poly-FPs in the reaction mixture. The analysis of the poly-FP mixtures by electrospray source ionization mass spectrometry with positive mode, ESIMS (+), accounts for the formation of mono-, bis-, tris-, and tetrasubstituted derivatives (see Experimental Section).

Table 4. MW-assisted azomethine ylide cycloaddition to [60]fullerene in [omim]BF_4/o-DCB = 1/3. Reaction scope explored in the presence of sarcosine and different aldehydes.

Entry[a]	Aldehyde	Ratio[b]	Conv. [%][c]	Mono-FP [%][d]	Selectivity[e]
1[f]	1	2/4	61	41	2.1
2[f]	2	2/4	90	23	0.3
3[f]	3	2/4	61	51	4.9
4[f]	4	2/4	62	46	2.9
5[g]	1	10/20	95	4	0.04
6[g]	2	10/20	98	–	–
7[g]	3	10/20	81	5	0.07
8[g]	4	10/20	69	23	0.5

[a] In all reactions: [60]fullerene 0.14 mmol; [omim]BF_4/o-DCB = 1/3; MW irradiation at 12 W, T_{bulk} = 100 °C, under magnetic stirring and simultaneous cooling by compressed air. [b] Added equivalents with respect to [60]fullerene. [c] [60]Fullerene conversion monitored by HPLC analysis. [d] % of mono-FP monitored by HPLC analysis. [e] Mono-FP/poly-FP ratio. [f] Reaction performed in 1.0 mL for 2 min. [g] Reaction performed in 0.5 mL for 10 min.

The MW-assisted protocol has been also applied to the synthesis of the novel fluorous-tagged FP **4**. Due to the presence of a C_2H_4 aliphatic spacer, the fluorinated aldehyde shows a similar reactivity to the parent heptaldehyde. Mono-FP **4** has been isolated in 30% yield and characterized by ^{1}H-, ^{19}F-, ^{13}C-NMR, ESIMS, FTIR, and UV/Vis spectroscopies. It is worth mentioning that the poly-FP **4** mixture displays a remarkable solubility in fluorinated alcohols, such as trifluoroethanol and hexafluoropropanol, which makes it interesting for photosensitized oxygenations in fluorous environments, as well as for applications in surface and membrane chemistry.[21]

Functionalization of carbon nanotubes in IL media under MW irradiation: The combined use of MW activation and ILs provides a new strategy for the functionalization of as-produced, non-oxidized SWNTs by the 1,3-dipolar cycloaddition of azomethine ylides. In the present work, we explore the use of the so-called "bucky gels", as reaction media, when exposed to reagents and to MW irradiation. We tested three different ILs, namely [bmim]BF_4, [omim]BF_4, and [hvim][$(CF_3SO_2)_2N$], to evaluate the influence of the length of the alkyl chain (4, 8, or 16 carbon atoms, respectively) and of the presence of an additional π bond ([hvim][$(CF_3SO_2)_2N$]) on the SWNT exfoliation ability and cycloaddition promotion. The exfoliation ability was investigated through rheological measurements at 25 and 60 °C in order to study the changes in stability, consistency, and degree of the IL coating on the SWNT by varying the IL nature and temperature. Indeed, the affinity of the ILs for the SWNT surface is fundamental for the formation of the gels, as pure ILs do not possess any elastic component. Rheological measurements, in the dynamic mode at a constant shear stress, indicate a viscoelastic gel-like behavior for the investigated IL/SWNT mixtures with the measured storage moduli (elastic, G') dominating the loss moduli (viscous, G'') by one order of magnitude and exhibiting little frequency dependence over the range of angular frequencies tested.

Table 5. Rheological characterization of the IL-SWNT gels.

IL[a]	G' [Pa][b] at 25 °C (at 60 °C)	G'' [Pa][b] at 25 °C (at 60 °C)	η^* [cP][b,c] at 25 °C (at 60 °C)	τ_y [Pa] at 25 °C (at 60 °C)	η [cP][d] at 25 °C (at 60 °C)
[bmim]BF_4	550 (300)	55 (50)	8.9×10^5 (4.3×10^5)	12 (5)	5000 (1000)
[omim]BF_4	800 (200)	80 (50)	13×10^5 (3.6×10^5)	25 (4)	7200 (1800)
[hvim][$(CF_3SO_2)_2N$]	(2500)	(400)	(43×10^5)	(9)	(2400)

[a] Pure [bmim]BF_4, [omim]BF_4, and [hvim]][$(CF_3SO_2)_2N$] have a viscosity of 80 cP at 25 °C and 70 cP at 60 °C, 240 cP at 25 °C and 200 cP at 60 °C, and 200 cP at 60 °C, respectively. [b] Shear stress (τ) 1.0 Pa satisfying the linear viscoelasticity; angular frequency (ω) varied from 0.1 to 10 Hz. [c] Calculated at the frequency of 0.1 Hz. [d] Calculated at $\gamma = 10\ s^{-1}$.

These results are indicative of systems that possess elastic and permanent networks. However, these gels lose their elastic properties at a relatively low value of shear stress (τ_y) (see Table 5) and show, during measurements in the static mode (see Figure S8 in the Supporting Information), a shear thinning behavior with a leveling off of the viscosity (η) to a minimum plateau value at shear rates of about $10\ s^{-1}$. This piece of evidence highlights the existence of weak interactions within the gel, and excludes the possibility that the rheological behavior is governed by the high intermolecular cohesive forces (as high as $0.5\ eV\,nm^{-1}$) between SWNTs characterizing their entanglement.[11] On the other hand, such interactions point to a large number of weak physical crosslinks between the SWNT bundles mediated by ILs. As a matter of fact, cation–π interactions, and also weaker π–π interactions, between alkylimidazolium cations and the sp^2 carbon framework of SWNTs may orient and trigger clustering of the surrounding imidazolium ions and consequently interconnect neighboring SWNTs. In addition, an increase in the temperature (from 25 to 60 °C) generates a decrease of the viscosity and also a further reduction of the shear stress. As far as the comparison of the investigated gels is concerned, the trend of the complex viscosity η^*, of the elastic modulus and of the steady shear viscosity, η, follow approximately the order [hvim][$(CF_3SO_2)_2N$] > [omim]BF_4 ≥ [bmim]BF_4. The higher the values of G' and G'', the greater the number of interactions and/or the stronger the interactions within the gel.[22] These results point to the fact that, besides the prevailing cation–π interactions as already highlighted elsewhere,[11] Van der Waals interactions between the ILs and the SWNT surface, due to the presence of the alkyl chains on the imidazolyl group, do affect the viscosity of the bucky gels and the ability of the investigated ILs to exfoliate SWNTs. The better performance of [hvim][$(CF_3SO_2)_2N$] at SWNT debundling is probably due to its higher polarizability (thanks to both its long alkyl chain and extra double bond), which renders it capable of interacting favorably with the CNT surface through stronger dispersion forces, which help to overcome the inter-SWNT attraction.

Functionalization of bucky gels: The gel phase provides the CNT with a uniform coating of IL film, which favors exfoliation and assists the modification of the carbon surface (Scheme 2).[23] In this scenario, the pseudo-supported IL layer acts as a sort of extracting medium to: 1) solubilize and transfer the starting reagents; 2) promote the in situ formation of active intermediates; and 3) stabilize uphill pathways and transition states.

Furthermore, the IL matrix sets forward a molecular heater array, under MW irradiation, to foster a flash and highly efficient thermal activation for endothermal processes. With this aim, we have investigated the 1,3-dipolar addition of azomethine ylides to SWNTs in IL-structured gels (Table 6). In the first instance, the degree of CNT functionalization (i.e. the number of attached functions per carbon atom of the nanotube) was established by thermogravimetric analysis (TGA), which enables evaluation of the total mass loss as derived from the functional groups covalently attached to the CNT surface, after subtraction of the pristine SWNT contribution. The functionalized SWNTs were further characterized with a variety of techniques, including Raman, UV/Vis/NIR spectroscopies, and transmission electron microscopy (TEM). The MW-assisted protocol was compared with the conventional synthesis in either molecular solvent (DMF) or [bmim]BF_4, performed for five days at 120 °C (entries 1 and 2 in Table 6).

Notably, MW irradiation, for 1 h, and with an applied power of 20 W, is instrumental for good to excellent functionalization of SWNTs, yielding group coverages up to

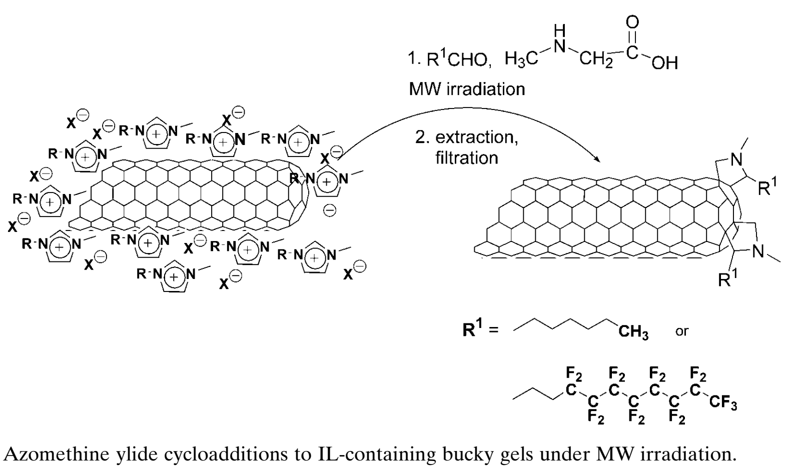

Scheme 2. Azomethine ylide cycloadditions to IL-containing bucky gels under MW irradiation.

Table 6. MW-assisted azomethine ylide cycloaddition to SWNTs in IL.

Entry[a]	Aldehyde	Solvent, T[b]	TGA wt loss [%][c]	N[d]
1[e]	CH_3-$(CH_2)_5$CHO	DMF, 120 °C	7	1/164
2[e]	CH_3-$(CH_2)_5$CHO	[bmim]BF_4, 120 °C	7	1/156
3[f]	CH_3-$(CH_2)_5$CHO	[bmim]BF_4, MW	9	1/120
4[f]	CH_3-$(CH_2)_5$CHO	[omim]BF_4, MW	6	1/191
5[f]	CH_3-$(CH_2)_5$CHO	[hvmim][$(CF_3SO_2)_2N$], MW	0	0
6[f,g]	CH_3-$(CH_2)_5$CHO	[bmim]BF_4/*o*-DCB, MW	16	1/60
7[f,h]	C_8F_{17}-$(CH_2)_2$CHO	[bmim]BF_4, MW	14	1/239
8[f,i]	C_8F_{17}-$(CH_2)_2$CHO	[bmim]BF_4, MW	16	1/211
9[h,j]	C_8F_{17}-$(CH_2)_2$CHO	[bmim]BF_4, MW	27	1/108

[a] In all reactions: SWNT Carbon Nanotechnologies Incorporated, 5–10 mg; sarcosine 1.0 mmol; aldehyde 2.0 mmol. [b] Solvent or IL gel and conditions with conventional heating (°C) or MW irradiation under magnetic stirring and simultaneous cooling by compressed air (MW). [c] % Weight loss determined by thermogravimetric analysis. [d] SWNT functionalization coverage per carbon atom. [e] Sarcosine 0.2 mmol, aldehyde 0.2 mmol, 5 day reaction. [f] 20 W, $T_{bulk} = 120$ °C, 1 h. [g] [omim]BF_4/*o*-DCB = 1/3. [h] Aldehyde 0.2 mmol, sarcosine 0.2 mmol. [i] aldehyde 0.5 mmol, sarcosine 0.5 mmol. [j] 50 W, $T_{bulk} = 140$ °C, 1 h.

1/60. This result represents one step forward in the chemistry of CNTs, as far as product yields and reaction time are concerned.[6]

Moreover, under the conditions adopted, the bucky gels respond properly to MW absorption, with a well-behaved and reproducible temperature/pressure rise profile, so that the scaling up of the synthesis is feasible with a controlled and safer reaction setup. It is known that pristine SWNTs, under solvent-free MW irradiation, undergo intense heat release in conjunction with uncontrolled spark emission and ignition phenomena. In a dense/viscous solvent environment, such highly effective MW absorption is prevented, but also the flash MW-induced thermal activation is suppressed.[6] In this light, the bucky-gel matrix does represent a powerful alternative, as the IL medium shields the strong SWNT response, while providing a safer source of instant heating, by virtue of its fully ionic character.

The data in Table 6 allow us to address the impact of the IL nature and of *o*-DCB as cosolvent on the reaction efficiency. In particular, an increased performance is registered in low viscosity bucky gels. Indeed, the functionalization coverage decreases in the order [bmim]BF_4 > [omim]BF_4 > [hvim]TF_2N (entries 3–5, Table 6), thus ranking the ILs in the reverse order with respect to the viscosity determination (see previous paragraph). The different abilities of the investigated bucky gels to function as solvents for the dipolar cycloaddition probably stem from the different mesoscopic structures of the gels formed. Indeed, many gels contain domains with microviscosities close to those of the neat liquid components (the ILs in this case),[24] leading to relatively short translational diffusion coefficients despite a very high macroscopic viscosity. Indeed, in the present cases, the measured G' and G'' moduli clearly highlight increased interactions within the gel on increasing the length of the alkyl chain, with [hvim][$(CF_3SO_2)_2N$] being the IL characterized by the greatest number of interactions and/or the strongest interactions. Therefore, in the latter case, the mobility of one or more reactants might be particularly reduced, for example, by selective entrapment in the gel network, to an extent adversely affecting the reaction rate.

In agreement with what is observed for the parent [60]fullerene, the addition of *o*-DCB as a co-solvent brings about a substantial improvement of the SWNT functionalization yield (entry 6, Table 6). Besides the TGA result, this is unequivocally confirmed by the time evolution of the Raman spectra, collected with excitation at 632.8 nm, of the treated SWNT by MW irradiation under the reaction conditions (Figure 2). Comparison with the Raman features of the starting material, which show a small defect mode at 1314 cm^{-1}, points to a gradual increase of this band, corresponding to the functionalization progress. Inspection of the radial breathing mode (RBM) spectral region (< 400 cm^{-1}) in the Raman spectrum provides direct evidence that the applied MW-assisted protocol is not affecting the overall distribution of the nanotube types. As a further remark, the partial loss of the characteristic interband transitions between van Hove singularities of SWNTs is also consistent with the occurrence of their functionalization (Figure 3). TEM images indicate that the nanotube bundles are highly dispersible in polar organic solvents such as DMF (Figure 4 and Figure S10 in Supporting Information).

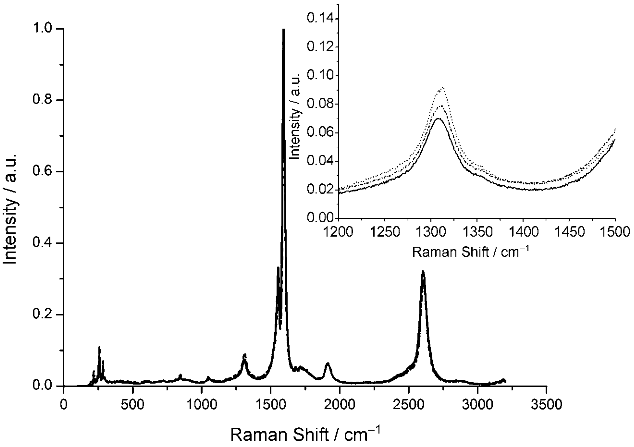

Figure 2. Time evolution of Raman spectra collected for pristine SWCNTs (CNI) (solid line) and for CNT derivatives obtained as reported in Table 6: entries 3 (dash-dot line) and 6 (dashed line). In the inset, the increase of the D band is visible: the higher the functionalization, the higher the D band in the Raman spectrum.

The rational explanation for the enhanced efficiency observed with the molecular cosolvent is probably twofold, and not only related to solubilization/diffusion effects, but also due to the parallel inhibition of the competitive retro-cycloaddition process. Indeed, pyrrolidine cycloreversion has been demonstrated also in the case of covalently modified SWNTs, under thermal and catalytic conditions.[6a]

As in the case of [60]fullerene, the MW-assisted protocol has been applied to the introduction of fluorous-tagged pyrrolidine moieties onto the SWNT surface (entries 7–9,

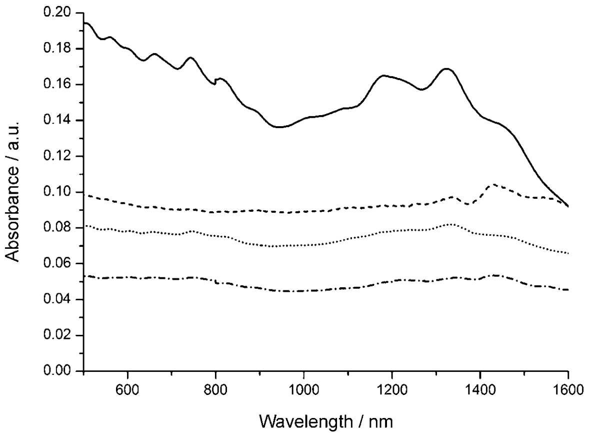

Figure 3. UV/NIR spectra in DMF of SWCNTs (CNI) (solid line) and of CNT derivatives obtained as reported in Table 6: entries 1 (dotted line), 3 (dash-dot line), and 6 (dashed line).

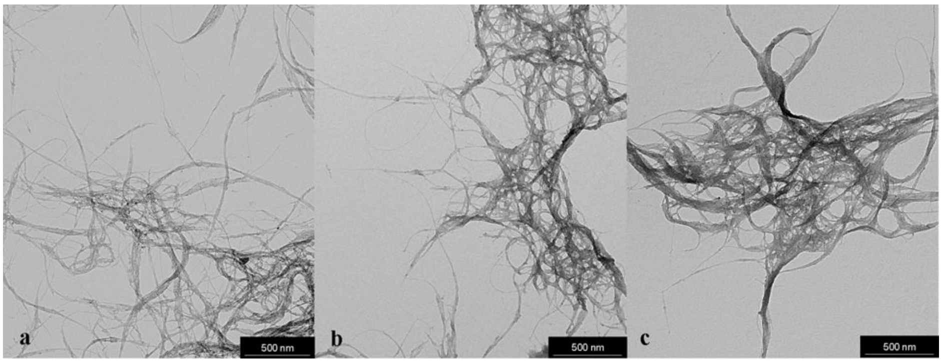

Figure 4. TEM images of functionalized CNT derivatives obtained as reported in Table 6 [entries 2 (a), 3 (b), 6 (c)] and dispersed in DMF.

Table 6). Interestingly a 1/108 functional coverage is obtained by using a lower excess of the fluorous-tagged aldehyde, at an applied MW power of 50 W. The resulting material features an unprecedented affinity for fluorinated phases. Solutions of up to 1 mg in hexafluoroisopropanol (1 mL) remain stable for weeks, without showing appreciable material precipitation. TGA data, Raman spectra, and TEM images provide converging evidence of the expected functionalization (see the Supporting Information).

Conclusions

An innovative strategy for the functionalization of CNS has been designed by the combined use of IL phases and MW irradiation. Under the conditions explored, azomethine ylide cycloaddition to [60]fullerene occurs smoothly in just 2–10 min. The same procedure has been successfully applied to SWNTs. Here, the use of IL-structured bucky gels as reaction media allows a controlled flash thermal activation induced by MW absorption, providing a straightforward tool for the covalent functionalization of the SWNT surface.

The easy access to novel CNS-based materials with a broader range of properties may be envisaged, and, in the present work, we have proven that interesting fluorous-tagged derivatives can be prepared in a very simple way.

Experimental Section

General: ^{1}H and ^{19}F NMR spectra were recorded at 298 K on a Bruker Avance DRX 400 spectrometer, operating, respectively, at 400.13 and 376.50 MHz. δ values in ppm are relative to $SiMe_4$ and $C_6H_5CF_3$. $^{13}C\{^1H\}$ NMR spectra were recorded at 298 K on a Bruker AC250 spectrometer operating at 62.9 MHz. δ values in ppm are relative to $SiMe_4$. ESIMS (+) spectra were collected with a Agilent LC/MSD Trap SL instrument. UV/Vis spectra were recorded on a Perkin–Elmer Lambda 45 spectrophotometer using quartz cells with 1 mm path length. Micro-Raman spectra were recorded with an inVia Renishaw spectrometer equipped with a He–Ne (632.8 nm) laser. UV/NIR spectra were recorded in 1 cm quartz cuvettes on a Varian Cary 5000 spectrophotometer. FTIR (KBr) spectra were collected by using a Nicolet 5700 instrument. The thermogravimetric analyses were performed with a TGA Q500 (TA Instruments) at 10 °C min^{-1} under N_2. For the TEM analyses, a small amount of the functionalized SWNTs was suspended in DMF, and a drop of the suspension was placed on a copper grid (3.00 mm, 200 mesh, coated with carbon film). After being air-dried, the sample was investigated by TEM Philips EM 208, with accelerating voltage of 100 kV. Continuous microwave irradiation was carried out in a CEM-Discover monomode microwave apparatus, with simultaneous monitoring of irradiation power, pressure, and temperature. Compressed air was applied to improve the temperature control of the reaction mixtures. All reactions were monitored by HPLC, using a Shimadzu LC-10AT VP pump system, equipped with a UV detector SPD-10 A VP set at 340 nm. HPLC analysis was performed with Phenomenex Luna and Cosmosil Buckyprep columns: (250 × 4.6 mm, 5 μm particles).

Fulleropyrrolidines **1**–**3** and the fluorous-tagged aldehyde CF_3-$(CF_2)_7CH_2CH_2CHO$ were prepared following literature procedures.[2,25] Generally, sarcosine (50 mg, 0.56 mmol) and the aldehyde (1.12 mmol) were added to a solution of fullerene (200 mg, 0.28 mmol) in toluene (150 mL). The reaction mixture was heated under reflux for 5 h. Then the solution was reduced in volume and the crude product was purified by flash column chromatography. All the spectral features were in agreement with the expected structures.

Mono-FP 4: Yield: 60 mg, 30 %. Soluble in C_6H_6, $C_6H_5CH_3$, $CHCl_3$. $R_f=$ 0.84 (toluene); ^{1}H NMR (400.13 MHz, C_6D_6, 25 °C, TMS): $\delta=4.28$ (d, ^2J(H,H) = 9.84 Hz, 1 H), 3.66 (d, ^2J(H,H) = 9.89 Hz), 3.60 (m, 1 H), 2.65–2.54 (m, 4 H, CH_2CH_2), 2.43 ppm (s, 1 H; CH_3); ^{19}F NMR (376.47 MHz, C_6D_6, 25 °C, $C_6H_5CF_3$): $\delta=-86.4$ (t, ^3J(F,F) = 9.64 Hz, 3F), −119.5 (m, 2F), −126.9 (m, 2F), −127.2 (m, 4F), −128.1 (m, 2F), −128.5 (m, 2F), −131.6 ppm (m, 2F); ^{13}C NMR ($CDCl_3$:CS_2 = 8:2, 25 °C, TMS): $\delta=$ 146.18, 146.13, 146.07, 146.01, 145.97, 145.93, 145.90, 145.86, 145.83, 145.52, 145.50, 145.44, 145.35, 145.31, 145.23, 145.20, 145.17, 145.15, 145.09, 144.58, 144.36, 144.26, 144.18, 143.08, 142.95, 142.59, 142.56, 142.51, 142.03, 141.98, 141.97, 141.94, 141.90, 141.86, 141.82, 141.70, 141.64, 140.25, 140.09, 139.97, 139.79, 137.08, 135.91, 135.71, 135.14 77.21, 75.47, 76,06, 69.94, 39.57 , 27.44 (t, ^2J(C,F) = 22.2 Hz, CH_2CF_2), 20.61 ppm ($CH_2CH_2CF_2$) (signals for C-F nuclei, expected between 125 and

105 ppm, cannot be detected due to their low intensity, resulting from J(C,F) scalar couplings); FTIR (KBr): $\tilde{\nu}=2961$, 2922, 2851, 2783, 1261, 1239, 1205, 1146, 1133, 1097, 1028, 804, 704, 574, 554, 527 cm^{-1}; UV/Vis ($CDCl_3$): λ_{max} (ε) = 254 (64960), 308 (21434), 427 (2079), 430 (3347), 700 nm (317 $mol^{-1}dm^3cm^{-1}$); ESIMS (+) (CH_2Cl_2:CH_3OH = 1:1, CF_3CO_2H 0.01 %): m/z: calcd for $C_{73}H_{11}F_{17}N^+$: 1223.9; found: 1223.9.

Procedure for MW-assisted synthesis of FPs: Unless otherwise stated, fullerene (5 mg, 0.07 mmol) was dispersed upon sonication in a mixture of ionic liquid and *o*-dichlorobenzene, together with sarcosine (1.2 mg, 0.14 mmol) and the aldehyde (0.28 mmol), in a closed glass test tube. Continuous microwave irradiation was carried out with simultaneous monitoring of irradiation power, pressure, and temperature. Samples were diluted using *o*-dichlorobenzene and analyzed by HPLC. Retention times of the corresponding monoderivatives are the following: (HPLC, Phenomenex Luna, toluene/n-hexane 4/1): 7.4 (**1**), 3.9 (**2**), 9.2 (**3**), 4.1 (**4**) min. Mono- and poly-FPs **2** have been characterized by ESIMS(+), in CH_2Cl_2:CH_3OH = 1:1, CF_3CO_2H 0.01 %, as follows: mono-FP **2**: m/z: calcd for $C_{79}H_{16}N^+$: 978.1; found: 978.2; bis-FP **2**: m/z: calcd for $C_{98}H_{31}N_2^+$: 1236.2; found: 1236.2; tris-FP **2**: m/z: calcd for $C_{117}H_{46}N_3^+$: 1493.4; found: 1493.3; tetra-FP **2**: m/z: calcd for $C_{136}H_{61}N_4^+$: 1750.5; found: 1750.4.

Bucky gel preparation: The proper amount of purified and unpurified HiPCO SWNTs was poured in an agate mortar and ground for 30 min with 1 mL (or 1 g in the case of solid IL) of the ionic liquid. The obtained suspension was poured into a vessel and sonicated using an ultrasonic bath sonicator (Bandelin Sonorex, 35 KHz) for 1 h. The sonication increases the apparent viscosity of originally liquid samples. [Hvim][$(CF_3SO_2)_2N$] is solid at room temperature. Therefore, the grey powder obtained by 30 min grinding in the mortar was poured into a vessel and heated at 50 °C before sonication. The obtained sample was either used for synthetic purposes or poured in the rheometer for the rheological measurements. No centrifugation step was performed in order to remove excess IL. The samples appeared to be quite stable for a few weeks, and did not tend to separate into a black gel phase and a transparent liquid phase within this time frame.

Rheology: Static and dynamic measurements were performed on a Thermo Scientific modular rheometer Haake M.A.R.S. II equipped with an Electron Corporation thermocontroller system Haake Phoenix (data evaluation: RheoWin software 3.61) using the cone plate geometry (cone diameter 6 mm, angle 0.5°). All samples, subjected to vacuum pumping before measurements, were directly loaded onto the plate of the rheometer and were allowed to equilibrate for only 6 min. As a matter of fact we did not pre-stress the samples or allow a longer equilibration time, because this would have required the samples to be left undisturbed between the plates for around 24 h, and this delay would have favored the undesired hydration of the ionic liquids. The shear stress sweep tests showed that 1.0 Pa satisfies the linear viscoelasticity for all samples. The dynamic storage and loss moduli were examined in the linear viscoelastic regime at 25 °C unless otherwise stated.

Procedure for the MW-assisted functionalization of bucky gels: Unless otherwise stated, 5 mg of HiPCO purified SWCNTs, used as received from CNI, were dispersed in the IL and mixed with sarcosine (1 mmol) and aldehyde (2 mmol). The reactions were carried out in closed glass test tubes with stirring, under microwave irradiation, as detailed in the Supporting Information. The reaction mixtures were cooled down to room temperature and then suspended in DMF. Afterwards they were filtered through a Millipore filter (JH 0.45 mm). The resulting material was washed on the filter with DMF and diethyl ether and recovered, then it was resuspended in DMF upon sonication for 20 min. It was refiltered, rewashed on the filter with DMF and diethyl ether, and at this point the collected black material was suspended in acetone and sonicated for 20 min in order to remove all the ILs. Finally, it was filtered again, and washed on the filter with acetone and diethylether. Thermal reactions, with and without ILs, were carried out for comparison purposes, by heating analogue mixtures in closed vials using an oil bath.

Acknowledgements

We thank Prof. Moreno Meneghetti (Nanophotonics Laboratory, University of Padova, Dept. of Chemical Sciences) for assistance with Raman spectroscopy. This work was carried out with support from the Universities of Padova (Progetto Strategico 2008, HELIOS, prot. STPD08RCX), Trieste, and Chieti, ITM-CNR, INSTM, MIUR (PRIN 2006, prot. 200634372 and FIRB, prot. RBNE033 KMA).

---

[1] a) A. Hirsch, M. Bettreich, *Fullerenes: Chemistry and Reactions*, Wiley-VCH, Weinheim, **2005**; b) D. Bonifazi, O. Enger, F. Diederich, *Chem. Soc. Rev.* **2007**, *36*, 390–414; c) C. C. Thilgen, F. Diederich, *Chem. Rev.* **2006**, *106*, 5049–5135.

[2] a) M. Maggini, G. Scorrano, M. Prato, *J. Am. Chem. Soc.* **1993**, *115*, 9798–9799; b) M. Prato, M. Maggini, *Acc. Chem. Res.* **1998**, *31*, 519–526; c) N. Tagmatarchis, M. Prato, *Synlett* **2003**, 768–779.

[3] a) M. Prato, *J. Mater. Chem.* **1997**, *7*, 1097–1109; b) M. Prato, *Top. Curr. Chem.* **1999**, *199*, 173–187; c) A. Mateo-Alonso, C. Sooambar, M. Prato, *Org. Biomol. Chem.* **2006**, *4*, 1629–1637; d) A. Mateo-Alonso, D. M. Guldi, F. Paolucci, M. Prato, *Angew. Chem.* **2007**, *119*, 8266–8272; *Angew. Chem. Int. Ed.* **2007**, *46*, 8120–8126.

[4] a) F. Langa, P. de La Cruz, *Comb. Chem. High Throughput Screening* **2007**, *10*, 766–782; b) F. Langa, P. de La Cruz in *Microwaves in Organic Synthesis* (Ed.: A. Loupy), Wiley-VCH, Weinheim, **2002**, and references therein.

[5] a) P. de La Cruz, A. de La Hoz, F. Langa, B. Illescas, N. Martin, *Tetrahedron* **1997**, *53*, 2599–2608; b) S. Wang, J. Zhang, L. Song, H. Jiang, S. Zhu, *J. Fluorine Chem.* **2005**, *126*, 349–353; c) J. J. Oviedo, P. de La Cruz, J. Garín, J. Orduna, F. Langa, *Tetrahedron Lett.* **2005**, *46*, 4781–4784; d) H. Zeng, T. Wang, A. S. D. Sandanayaka, Y. Araki, O. Ito, *J. Phys. Chem. A* **2005**, *109*, 4713–4720.

[6] a) F. G. Brunetti, M. A. Herrero, J. de M. Muñoz, A. Díaz-Ortiz, J. Alfonsi, M. Meneghetti, M. Prato, E. Vázquez, *J. Am. Chem. Soc.* **2008**, *130*, 8094–8100; b) F. G. Brunetti, M. A. Herrero, J. de M. Muñoz, S. Giordani, A. Díaz-Ortiz, S. Filippone, G. Ruaro, M. Meneghetti, M. Prato, E. Vázquez, *J. Am. Chem. Soc.* **2007**, *129*, 14580–14581; c) X. Lu, F. Tian, X. Xu, N. Wang, Q. Zhang, *J. Am. Chem. Soc.* **2003**, *125*, 10459–10464; d) Y. Wang, Z. Iqbal, S. Mitra, *Carbon* **2005**, *43*, 1015–1020; e) J. Li, H. Grennberg, *Chem. Eur. J.* **2006**, *12*, 3869–3875.

[7] a) M. A. P. Martins, C. P. Frizzo, D. N. Moreira, N. Zanatta, H. G. Bonacorso, *Chem. Rev.* **2008**, *108*, 2015–2050; b) *Ionic Liquids in Synthesis* (Eds.: P. Wasserscheid, T. Welton), Wiley-VCH, Weinheim, **2003**.

[8] a) N. E. Leadbeater, H. M. Torenius, H. Tye, *Comb. Chem. High Throughput Screening* **2004**, *7*, 511–528; b) J. Habermann, S. Ponzi, S. V. Ley, *Mini-Rev. Org. Chem.* **2005**, *2*, 125–137; c) C. Guerrero-Sanchez, R. Hoogenboom, U. S. Schubert, *Chem. Commun.* **2006**, 3797–3799.

[9] a) Z. Yinghuai, S. Bahnmueller, C. Chibun, K. Carpenter, N. S. Hosmaneb, J. A. Maguirec, *Tetrahedron Lett.* **2003**, *44*, 5473–5476; b) J. A. Maguirec, Z. Yinghuai, *J. Phys. Chem. Solids* **2004**, *65*, 349–353.

[10] R. R. Deshmukh, J. W. Lee, U. S. Shin, J. Y. Lee, C. E. Song, *Angew. Chem.* **2008**, *120*, 8743–8745; *Angew. Chem. Int. Ed.* **2008**, *47*, 8615–8617.

[11] T. Fukushima, A. Kosaka, Y. Ishimura, T. Yamamoto, T. Takigawa, N. Ishii, T. Aida, *Science* **2003**, *300*, 2072–2074.

[12] a) T. Fukushima, K. Asaka, A. Kosaka, T. Aida, *Angew. Chem.* **2005**, *117*, 2462–2465; *Angew. Chem. Int. Ed.* **2005**, *44*, 2410–2413; b) I. Takeuchi, K. Asaka, K. Kiyohara, T. Sugino, N. Terasawa, K. Mukai, T. Fukushima, T. Aida, *Electrochim. Acta* **2009**, *54*, 1762–1768.

[13] H. B. Kim, J. S. Choi, S. T. Lim, H. J. Choi, H. S. Kim, *Synth. Met.* **2005**, *154*, 189–191.

[14] B. K. Price, J. L. Hudson, J. M. Tour, *J. Am. Chem. Soc.* **2005**, *127*, 14867–14870.

[15] a) S. Berardi, M. Bonchio, M. Carraro, V. Conte, A. Sartorel, G. Scorrano, *J. Org. Chem.* **2007**, *72*, 8954–8957; b) M. Carraro, L. Sandei, A. Sartorel, G. Scorrano, M. Bonchio, *Org. Lett.* **2006**, *8*, 3671–3674.
[16] a) D. Tasis, N. Tagmatarchis, A. Bianco, M. Prato, *Chem. Rev.* **2006**, *106*, 1105–1136; b) W.-F. Chen, J.-S. Wu, P-L. Kuo, *Chem. Mater.* **2008**, *20*, 5756–5767; c) J. Zhang, L. Gao, J. Sun, Y. Liu, Y. Wang, J. Wang, H. Kajiura, Y. Li, K. Noda, *J. Phys. Chem. C* **2008**, *112*, 16370–16376.
[17] I. Guryanov, A. Montellano López, M. Carraro, T. Da Ros, G. Scorrano, M. Maggini, M. Prato, M. Bonchio, *Chem. Commun.* **2009**, 3940–3942.
[18] a) S. Filippone, M. Izquierdo Barroso, Á. Martín-Domenech, S. Osuna, M. Solà, N. Martin, *Chem. Eur. J.* **2008**, *14*, 5198–5206; b) N. Martín, M. Altable, S. Filippone, A. Martín-Domenech, L. Echegoyen, C. M. Cardona, *Angew. Chem.* **2006**, *118*, 116–120; *Angew. Chem. Int. Ed.* **2005**, *44*, 110–114.
[19] H. Liu, G.-h. Tao, D. G. Evans, Y. Kou, *Carbon* **2005**, *43*, 1778–1785.
[20] T. Carofiglio, P. Donnola, M. Maggini, E. Rossi, M. Rossetto, *Adv. Synth. Catal.* **2008**, *350*, 2815–2822.
[21] a) M. Bonchio, M. Carraro, G. Scorrano, A. Bagno, *Adv. Synth. Catal.* **2004**, *346*, 648–654; b) M. Bonchio, M. Carraro, G. Scorrano, E. Fontananova, E. Drioli, *Adv. Synth. Catal.* **2003**, *345*, 1119–1126; c) M. Bonchio, M. Carraro, M. Gardan, G. Scorrano, E. Drioli, E. Fontananova, *Chem. Commun.* **2006**, 4533–4535.
[22] J. Y. Kim, D. K. Kim, S. H. Kim, *Eur. Polym. J.* **2009**, *45*, 316–324.
[23] a) W. Tu, J. Lei, H. Ju, *Chem. Eur. J.* **2009**, *15*, 779–784; b) B. Wu, D. Hu, Y. Kuang, B. Liu, X. Zhang, J. Chen, *Angew. Chem.* **2009**, *121*, 4845–4848; *Angew. Chem. Int. Ed.* **2009**, *48*, 4751–4754.
[24] A. Skrzypczak, P. Neta, *J. Phys. Chem. A* **2003**, *107*, 7800–7803.
[25] C. Rocaboy, W. Bauer, J. A. Gladysz, *Eur. J. Org. Chem.* **2000**, 2621–2628.

Received: May 26, 2009
Revised: August 4, 2009